NeuroImage 57 (2011) 45–54

Contents lists available at ScienceDirect

NeuroImage

journal homepage: www.elsevier.com/locate/ynimg

Longitudinal studies of ischemic penumbra by using ^{18}F-FDG PET and MRI techniques in permanent and transient focal cerebral ischemia in rats

M. Sobrado [a], M. Delgado [b], E. Fernández-Valle [c], L. García-García [b], M. Torres [d], J. Sánchez-Prieto [d], J. Vivancos [e], R. Manzanares [f], M.A. Moro [a], M.A. Pozo [b], I. Lizasoain [a,*]

[a] Departamento de Farmacología, Facultad de Medicina, Universidad Complutense de Madrid, Spain
[b] CAI de Cartografía Cerebral Instituto Pluridisciplinar, Universidad Complutense de Madrid, Spain
[c] CAI Resonancia Magnética Nuclear, Instituto Pluridisciplinar, Universidad Complutense de Madrid, Spain
[d] Departamento de Bioquímica, Facultad de Veterinaria, Universidad Complutense de Madrid, Spain
[e] Unidad de Ictus, Servicio de Neurología, Hospital La Princesa, Madrid, Spain
[f] Servicio de Radiodiagnóstico Sección Neurorradiología, Hospital La Princesa, Madrid, Spain

ARTICLE INFO

Article history:
Received 28 December 2010
Revised 26 March 2011
Accepted 21 April 2011
Available online 28 April 2011

Keywords:
Cerebral ischemia
Experimental stroke
Magnetic resonance imaging
Positron emission tomography
Early reperfusion

ABSTRACT

At present, the goal of stroke research is the identification of a potential recoverable tissue surrounding the ischemic core, suggested as ischemic penumbra, with the aim of applying a treatment that attenuates the growth of this area. Our purpose was to determine whether a combination of imaging techniques, including ^{18}F-FDG PET and MRI could identify the penumbra area.

Longitudinal studies of ^{18}F-FDG PET and MRI were performed in rats 3 h, 24 h and 48 h after the onset of ischemia. A transient and a permanent model of focal cerebral ischemia were performed. Regions of interest were located, covering the ischemic core, the border that progresses to infarction (recruited tissue), and the border that recovers (recoverable tissue) with early reperfusion.

Analyses show that permanent ischemia produces severe damage, whereas the transient ischemia model does not produce clear damage in ADC maps at the earliest time studied. The only significant differences between values for recoverable tissue, ^{18}F-FDG (84 ± 2%), ADC (108 ± 5%) and PWI (70 ± 8%), and recruited tissue, ^{18}F-FDG (77 ± 3%), ADC (109 ± 4%) and PWI (77 ± 4%), are shown in ^{18}F-FDG ratios. We also show that recoverable tissue values are different from those in non-infarcted tissue.

The combination of ^{18}F-FDG PET, ADC and PWI MRI is useful for identification of ischemic penumbra, with ^{18}F-FDG PET being the most sensitive approach to its study at early times after stroke, when a clear DWI deficit is not observed.

Introduction

According to the classical definition, the ischemic penumbra is an area surrounding the ischemic core in which metabolism is impaired, and cells are structurally intact but functionally silent (Astrup et al., 1977). Many different therapeutic approaches have been studied with the aim of avoiding the evolution of the penumbra towards a non-viable infarct core. Nevertheless, at the moment, the main strategy for stroke treatment is the reperfusion of ischemic tissue using thrombolysis with tissue plasminogen activator (t-PA) (Adams et al., 1996). This therapy is based on the existence of a therapeutic time window, which in humans varies between 3 and 4.5 h after the onset of symptoms (Hacke et al., 2008). This aspect is decisive in selecting patients suitable for thrombolytic stroke therapy due to the risk of hemorrhagic transformation (Kaur et al., 2004) and in saving the tissue for the functional recovery of the patient. Therefore, the identification of penumbra is of great importance not only for stroke outcome but also as a diagnostic target to extend the therapeutic window and as a target for neuroprotective and neurorepair treatments (Lo, 2008). In this context, many neuroimaging approaches have been used, such as Perfusion-Weighted Imaging (PWI) and Diffusion-Weighted Imaging (DWI) Magnetic Resonance (MR) mismatch, Positron Emission Tomography (PET) with ^{15}O tracers, and PET imaging of the uptake of ^{18}F-labeled-fluoromisonidazole, among others (Rohl et al., 2001; Takasawa et al., 2007; Thiel et al., 2001). However, there are still controversies on what the best approach is, leading us to consider the penumbra as an area which may require several methodological approaches for its identification.

PET imaging has been applied for metabolic–biochemical–molecular studies *in vivo* in a minimally invasive way; for this reason, it is an excellent tool for both research and clinical practice. Of note, neuroimaging with ^{15}O-labeled tracers is considered one of the best existing methods for detection of brain areas with reduced

* Corresponding author at: Departamento de Farmacología, Facultad de Medicina, Universidad Complutense de Madrid. Avda. Complutense s/n 28040 Madrid, Spain. Fax: +34 91 3941464.
E-mail address: ignacio.lizasoain@med.ucm.es (I. Lizasoain).

1053-8119/$ – see front matter © 2011 Elsevier Inc. All rights reserved.
doi:10.1016/j.neuroimage.2011.04.045

cerebral metabolic rate of oxygen use (Heiss and Sorensen, 2009). However, this type of tracer is not usually available in many hospitals. In contrast, −2-[^{18}F]-fluoro-2-deoxy-D-glucose (^{18}F-FDG) is the standard PET tracer with a short physical half-life (109.8 min) that is commonly used in clinical practice. In this context, oxidation of glucose is the main way for energy supplies in the brain and FDG is transported to tissue and phosphorylated to FDG-P but, unlike glucose, it does not undergo significant further metabolism. Thus, it is trapped in the brain tissue in a way directly related to the local cerebral metabolic rate for glucose. Small animal PET is an evolving technology that makes it possible to probe biological processes *in vivo*, helping to translate knowledge from animal models of diseases – such as stroke – to the patient. Specifically, small animal PET with ^{18}F-FDG is sensitive to metabolic changes that occur after ischemic brain injury (Lou et al., 2007). On the other hand, since PET imaging by itself does not provide good identification of brain structures due to spatial resolution in the order of 1.5 mm in small animal imaging (Bandera et al., 2006; Obenaus and Ashwal, 2008), the fusion of structural (MRI) and metabolic (PET) images may facilitate the observation of functional impairment.

We have therefore decided to perform a systematic study on the utility of several widely accessible methods used in the clinical practice for the detection of potentially recoverable brain tissue after an ischemic insult. Our objectives, using both a permanent and a mild transient model of focal cerebral ischemia, were (1) to describe the evolution of stroke using ^{18}F-FDG PET, DWI, PWI and T2-weighted (T2WI) MRI after ischemic onset in the same animal and (2) to define the characteristics of a tissue that does not progress to infarction when early reperfusion occurs, using ^{18}F-FDG, apparent diffusion coefficient (ADC) and cerebral blood flow (CBF).

Material and methods

Focal cerebral ischemia models

Male Fischer rats (250–300 g body weight; Harlan; Barcelona, Spain) (n = 17) were used in the study. All experimental protocols adhered to the guidelines of the Animal Welfare Committee of the Universidad Complutense (following EU directives 86/609/CEE and 2003/65/CE). Animals were housed individually under standard conditions of temperature and humidity and a 12 h light/dark cycle (lights on at 08:00) with free access to food and water.

Rats were anesthetized (isoflurane 1.5–2% in 100% oxygen) and underwent analgesia (metamizole 100 mg/kg ip). Body temperature was maintained at physiological levels with a heating pad during the surgical procedure and anesthesia recovery. The femoral artery was cannulated for continuous monitoring of arterial pressure and blood sampling. Analysis of pH and gasses in the blood was performed before and 15 min after occlusion as well as 10 min after surgery ended.

The surgical procedure was a variant of that described by Chen et al.(1986) and Liu et al.(1989). A small craniectomy was made over the trunk of the right middle cerebral artery (MCA) and above the rhinal fissure, and the artery was ligated with a 9–0 suture just before its bifurcation into the frontal and parietal branches. Complete interruption of the blood flow was confirmed under an operating microscope. Then, both common carotid arteries (CCA) were also occluded.

Two models of focal ischemia were used. The permanent cerebral ischemia model consisted of a permanent occlusion of right MCA (pMCAO), and of both CCA; after 75 min, the contralateral CCA was de-occluded to reduce animal death rate. The mild transitory cerebral ischemia model consisted of the occlusion of the right MCA (tMCAO) and in both CCA; after 75 min, the three vessels were de-occluded and reperfusion was observed by the microscope; sham-operated animals were used as control group (Fig. 1). The distal MCAO technique produced a cortical infarct.

Some animals were excluded, for several reasons: 2 rats due to the appearance of a contralateral infarct, 1 rat by the presence of respiratory difficulties and 1 rat due to unusual basal MRI. No spontaneous mortality was found after MCAO with these models.

Magnetic resonance imaging (MRI)

Before ischemia (basal) and 2, 24 and 48 h after the end of the surgery (Fig. 1), the rats were anesthetized with isoflurane 1.5–2% for MRI. The earliest time selected (2 h) is the minimum time required for total recovery of the animal after anaesthetization and surgical procedures for MCAO. During the MRI procedure, the animals were kept at 37 °C and a MR compatible respiration sensor was used to control the animals.

The MRI experiments consisted of three-dimensional T2WI, a series of DWI to calculate the ADC maps and a series of PWI to calculate CBF maps. The perfusion experiments were carried out using Arterial Spin Labeling (ASL) techniques without contrast agent injection.

All the MRI experiments were performed on a BIOSPEC BMT 47/40 (Bruker, Ettlingen, Germany) spectrometer operating a 4.7 T, equipped with a 11.2 cm actively shielded gradient system, capable of 200 mT/m gradient strength and 80 μs of rise time. A 7-cm birdcage radiofrequency coil was used for transmission and reception.

Three-dimensional T2WI were acquired using a rapid acquisition with relaxation enhancement (RARE) technique, with a repetition time (TR) = 1650 s, RARE factor = 16, and interecho interval = 10 ms, resulting in an effective echo time (TE) = 80 ms, the field of view (FOV) = 4 × 4 × 4 cm^3. The acquired matrix size was 128 × 128 × 64. These data were zero-filled to obtain a reconstructed matrix size of 128 × 128 × 128.

For the ADC calculation, a series of 3 DWI images were acquired using a spin-echo sequence with the following acquisition parameters: TE = 75 ms, TR = 2 s, diffusion weighting factor varied from b = 33.3 s/mm^2 to b = 2118.6 s/mm^2, matrix size = 128 × 128, FOV = 3.5 × 3.5 cm^2. The slice package for these experiments consisted of eight 1.5-mm-thick slices in the coronal plane interleaved by a 0.5-mm gap.

Perfusion studies using the ASL technique consisted of the acquisition and comparison of a flow-sensitive (slice-selective inversion recovery) and a flow-insensitive (non-selective inversion recovery) series. For this purpose a Flow-Sensitive Alternating Inversion-Recovery Echo Planar Imaging (FAIREPI) sequence was used. The parameters for both series were: TR = 12 s, TE = 51 ms, slice thickness = 2 mm, thickness of the selective inversion slice = 6 mm, FOV = 3.5 × 3.5 cm^2, acquired matrix size = 128 × 64. The acquired data were zero-filled to obtain a reconstructed matrix size of 128 × 128. A total of 22 Inversion Times between 15 ms and 4215 ms were obtained.

T2WI, DWI and PWI image analysis was performed using ParaVision 3.0.1 (Bruker, Ettlingen, Germany).

The ADC maps were calculated from the DWI series using the Image Sequence Analysis (ISA) tool of the ParaVision package.

The CBF maps were calculated from the ASL images. First, the T1 maps from selective and non-selective inversion recovery series were calculated using the ISA tool. Then, these T1 maps were transferred to a PC and the CBF value was calculated in each pixel from the formula $rCBF = \lambda((1/T1_{sel}) - (1/T1_{nosel}))$; where λ is the blood/brain partition coefficient, which represents the difference between water concentration between blood and tissue. In our case λ is set at 0.9. This calculation was carried out using Matlab 7.3 (MathWorks, Inc., Natick, Massachusetts, USA).

^{18}F-FDG positron emission tomography (PET) imaging

The regional glucose metabolism of the brain lesion was evaluated *in vivo* by ^{18}F-FDG small animals PET imaging in rats fasted for 8 h and

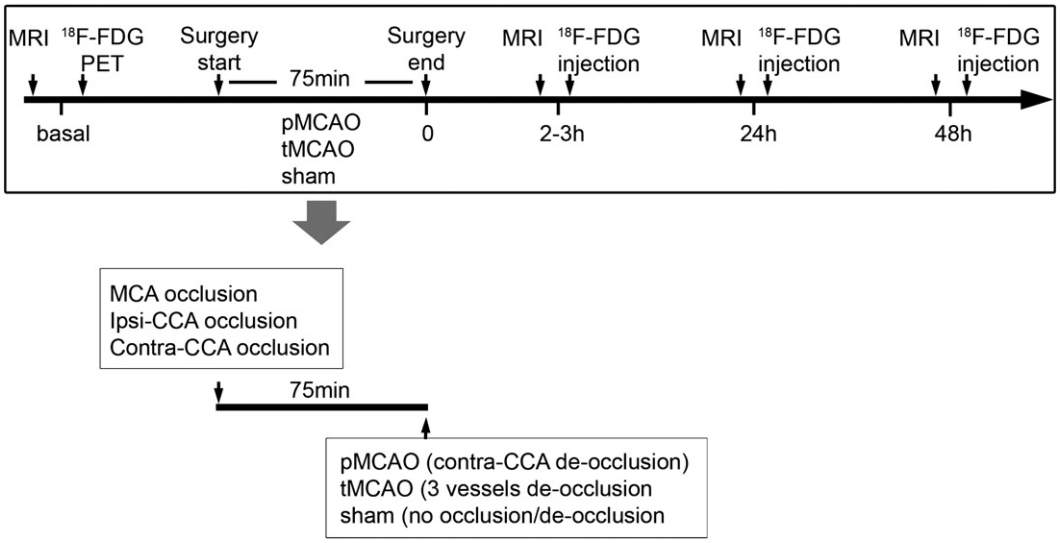

Fig. 1. Outline of the experiments providing an overview of the study. The time course followed in MRI and ^{18}F-FDG experiments after pMCAO and tMCAO focal cerebral ischemia and sham group in adult rat. pMCAO: permanent middle cerebral artery occlusion; tMCAO transient MCAO; CCAO: common carotid artery occlusion.

glycaemia was controlled. Immediately following MRI acquisition (Fig. 1), rats were injected intravenously with 18.5 MBq of ^{18}F-FDG through the tail vein. After an uptake period of 60 min, the animals were anesthetized (isoflurane 1.5% in 100% oxygen) and placed on the bed with the head centered in the field of view in a spread prone position and scanned with the Albira small animal PET scanner (Oncovision, Valencia, Spain). Body temperature was maintained at 36.5 ± 0.5 °C with a heating pad during the radiotracer incubation period. The scanner employs an innovative crystal design of only eight $40(50) \times 40(50) \times 9.8$ mm^3 LYSO tapered crystals forming detector modules read by position sensitive photomultipliers, providing a 8-cm transaxial and a 4-cm axial field of view, with image resolution <1.5 mm (Balcerzyk et al., 2009). A 60-min static acquisition was performed in three-dimensional mode. All the images were reconstructed using 3D Ordered Subset Expectation Maximization algorithm and dead time decay random and scatter corrections were applied. PET images were co-registered with MRI images (T2-3D) obtained from each rat. Briefly, the first step in the co-registration process was the automatic realignment of the volumetric T2WI3D MRIs of the same rat obtained at the different time points. Thereafter, 3D PET images were manually rotated and shifted to match them with their corresponding realigned MRIs. To this aim, the harderian glands from both PET and MRI scans were set as markers. In this process, a resolution adjustment was performed, to extrapolate the $80 \times 80 \times 80$ PET to $128 \times 128 \times 128$ MRI matrix. The trilinear interpolation algorithm was applied, which uses all 8 enclosing pixel values. All these steps were carried out by using PMOD v 2.9 software (PMOD technologies, Zurich, Switzerland).

Measurement of brain edema from MR images

Hypointensity regions from these ADC maps and hyperintensity regions on the T2WI images were outlined to evaluate the spatial development of the edema volume in all of the brain. These regions were manually drawn for each slice and the volume of cerebral edema was evaluated by calculating the total number of voxels corresponding to the edematous site throughout all image slices. Then the total volume of cerebral edema was expressed as the ratio between right cortical volume of lesion/right cortical volume in basal conditions (before ischemia; basal), multiplied by 100, for each animal using the data sets acquired at 2, 24 and 48 h after surgery.

Areas that exhibited increased T2WI signal intensity above of 125% of the normal tissue value in the contralateral hemisphere were recognized as vasogenic edema areas. In addition, areas with ADC values below 0.5×10^{-3} mm^2/s were interpreted as cytotoxic edema areas, with restricted diffusion of endogenous tissue water caused by cell death (Obenaus and Ashwal, 2008).

Definition of regions of interest (ROI)

After ^{18}F-FDG PET and 3D T2WI MRI images were co-registered, we selected two coronal slices, at the levels of bregma 0 and −2 mm, involving the right MCA territory and the area where the extent of cytotoxic and vasogenic edema at 24–48 h was the greatest and where it was always detected in all animals in both models. Then, these images were co-registered with ADC maps and CBF. Significant differences were not observed between the slices and therefore we showed the results of the slice bregma 0 (Rojas et al., 2006) for subsequent studies (Fig. 3A).

ROIs were manually drawn (Rojas et al.) over the ADC map image at the times indicated below to calculate ADC values. They were applied subsequently over the CBF maps, to calculate CBF, and over the PET, for the semiquantitative analysis of ^{18}F-FDG.

Two types of ROIs were established (Fig. 3): A first set of ROIs was defined to study the evolution of edematous tissue, for each model (pMCAO and tMCAO), as follows (Fig. 3B): i) ROI basal, corresponding to a cortical region in the MCA territory before the surgery; ii) ROI-NI (non-infarcted tissue), corresponding to a cortical, non-infarcted region in the ipsilateral hemisphere; iii) ROI-I (infarcted tissue), corresponding to the ischemic core, at 2–3 h (ROI-I_{3h}), 24 h (ROI-I_{24h}) and 48 h (ROI-I_{48h}). The tracing used for ROI-I_{3h} in tMCAO corresponds to the one delineated at 24 h in the same animal (ROI-I_{24h}) because, while tMCAO did not cause a detectable injury in ADC maps at early times (3 h) in the slices selected and in all animals, the lesion was clearly found at 24 h in all cases.

A second set of ROIs was selected for comparing areas of the two models, pMCAO and tMCAO, for definition of recruited and recoverable tissues, for which an initial ischemic damage was identical (75 min of occlusion of three vessels) but subsequently varied due to the presence (tMCAO) or absence (pMCAO) of reperfusion (Fig. 3C) of the three vessels. Thus, we defined i) ROI-NI, as before; ii) ROI-I, as the ischemic core, at 24 h for each rat subjected to tMCAO (ROI-$I_{24h\ tMCAO}$) and ROI-$I_{24h\ pMCAO}$, as the ischemic core average of all rats subjected to

pMCAO; iii) recruited tissue, an area that is not initially infarcted but will progress to infarction at 24 h with reperfusion; and iv) recoverable tissue, an area that will progress to infarction with the permanent occlusion of vessels but not with the reperfusion; it was calculated as recoverable tissue = ROI-$I_{24h\ pMCAO}$-ROI-$I_{24h\ tMCAO}$. ROIs drawn in the sham group were chosen from a random ischemic rat.

ADC, CBF MRI and ^{18}F-FDG PET data analyses

Relative values of cerebral metabolism were measured using ^{18}F-FDG uptake of each ROI. These values were normalized by the radioactive dose injected. The average ^{18}F-FDG uptake (Martin et al., 2009), ADC (Rojas et al., 2006) and perfusion for each ipsilateral ROI were calculated and expressed as the ratio to the symmetrical ROI in the homologous contralateral region and multiplied by 100.

Nissl staining

Animals subjected to permanent and transient focal cerebral ischemia were killed at 3 h after surgery by perfusion fixation with 4% paraformaldehyde in phosphate-buffered pH 7.4 and the brains were frozen, serially sectioned at 50 μm and stained with conventional histological Nissl (0.1% cresyl violet) staining.

Statistical analysis

All data were collected and analyzed in a triple blind manner. Statistics were performed using the GraphPad Prism software. The edema volumes were analyzed with a 2-way ANOVA followed by post hoc Bonferroni's test. For the time course of ADC, ^{18}F-FDG and CBF ratios in the infarcted areas, repeated measures ANOVA with Newman–Keuls test was used. One-way ANOVA and Newman–Keuls test was used to compare the difference in the ADC, CBF signal and ^{18}F-FDG at 2–3 h between ROI-NI, recruited tissue and recoverable tissue. Data are presented as mean ± SE. $P<0.05$ was considered significant.

Results

Physiological variables

The physiological variables studied were not significantly different between groups of animals before, during or after surgery. Physiological parameters (mean ± SD) after surgery ends were: mean arterial blood pressure 84.9 ± 9.5 *vs.*84.1 ± 3.2 mm Hg; blood pO2 184.5 ± 3.5 *vs.* 175.7 ± 14.3 mm Hg; pCO2 33.6 ± 2.0 *vs.* 33.4 ± 12.9 mm Hg; and pH 7.44 ± 0.01 *vs.* 7.46 ± 0.05 (pMCAO *vs.* tMCAO, respectively).

Study of the cerebral edema volume using ADC maps and T2WI in a permanent and a mild transient model of focal cerebral ischemia

We studied how early vascular reperfusion modifies the evolution of brain edema size, comparing a transient occlusion model with a permanent ischemic model. To do this, we expressed edema size as the percentage of the ipsilateral basal cortex size.

We found that total edema volume, measured on ADC maps and T2WI (Fig. 2), significantly increased from 2–3 to 24 h and then did not change until 48 h in both pMCAO and tMCAO focal cerebral ischemia models. The total edema volume was significantly larger in the permanent model than in the transient one at 24–48 h.

However, only ADC maps, but not T2WI, showed significant differences at 2–3 h in the edema, with greater differences in the pMCAO model. In fact, tMCAO did not produce a clear hypointensity signal in ADC maps a 2–3 h and showed a high variability (Fig. 2, A2, A5) when compared with pMCAO (Fig. 2, A1, A4). All animals in both models showed a clear lesion at 24 and 48 h in ADC maps and T2WI (Fig. 2B, C).

Study of the edematous tissue by using ^{18}F-FDG uptake, ADC and CBF in a permanent and a transient model of focal cerebral ischemia

Regions of interest were defined for each rat on ADC maps in the ipsilateral cortex to calculate the ^{18}F-FDG uptakes, ADC and CBF values, which were expressed as % of those found in symmetrical ROIs drawn in the homologous contralateral regions (Fig. 3B). The tracing used for ROI-I_{3h} corresponds to the one delineated at 24 h in the same animal (ROI-I_{24h}) because the tMCAO model did not produce a clear edema in ADC maps at 3 h.

In pMCAO, we found a significant decrease in the ^{18}F-FDG uptake in the ROI-1_{3h} corresponding to the ischemic core at 2–3 h after surgery, which further decreased at 24 h and 48 h after surgery (Fig. 4: A1). In tMCAO, there was also a metabolic activity reduction at all the times studied (Fig. 4: A2). The sham group did not show changes in ^{18}F-FDG uptake at the times studied (Fig. 4: A3).

The ADC ratios of the ischemic *vs.* the contralateral cortex are shown in Fig. 4B. We found a significant decrease in the ADC value of the ischemic core 2–3, 24 and 48 h after surgery in pMCAO and at 24 h in tMCAO but not in the sham group (Fig. 4: B1–B3). After pMCAO, the reduction in the ADC value was of a lesser extent 48 h after surgery (Fig. 4: B1).

The CBF ratios of the ischemic *vs.* the contralateral cortex are shown in Fig. 4C. We found a significant reduction in the CBF value of the ischemic core 2–3 h after surgery, which further decreased at 24 and 48 h after surgery in pMCAO (Fig. 4: C1). CBF was not significantly changed either in tMCAO or in the sham group (Fig. 4: C2–C3).

Histological outcome

In the pMCAO model, the injury area – seen at 3 h after surgery – shows a variable staining throughout the MCA territory combining: 1) areas with loss of cytoplasmic Nissl staining and rounded with swollen neuronal cells and 2) areas showing a triangular morphology with a reduced size of cell body and processes (Fig. 5A: A1–A2). Whereas, in the tMCAO model, most of the damaged cells – at 3 h after surgery –, appeared with a triangular morphology and marked condensed nucleus with irregular clumped chromatin (Fig. 5B: B1–B2).

Study of the recruited and recoverable tissue by using ^{18}F-FDG, ADC and CBF values in a transient focal ischemia model

In order to define the specific features of an area that is not initially infarcted and that will not progress to infarction if reperfused (recoverable tissue), we retrospectively studied ^{18}F-FDG uptake, ADC and CBF values in ROIs defined 24 h after surgery in both models (ROI-$I_{24h\ pMCAO}$, ROI-$I_{24h\ tMCAO}$) on images obtained at 2–3 h in the transient model. We used the ADC maps at 24 h since a clear hypointensity signal was observed at this time and the edema size was stable.

The ROIs corresponding to the ischemic tissue in ADC maps at 2–3 h in tMCAO those progresses to infarction at 24 h, even with reperfusion (recruited tissue), showed a significant reduction in ^{18}F-FDG uptake when compared with a border area that recovers with reperfusion (recoverable tissue). All these ROIs showed a lesser ^{18}F-FDG uptake than that found in the non-infarcted tissue (ROI-NI) (Fig. 6A). No significant changes in the ADC and CBF ratios were observed among all of the ROIs studied (Fig. 6B and C). A light CBF reduction was observed in the recoverable tissue but it did not reach statistical significance.

Discussion

To our knowledge, this is the first systematic comparison of two models of ischemia (permanent and transient) using longitudinal studies of ^{18}F-FDG PET and MRI aimed to define a recoverable tissue

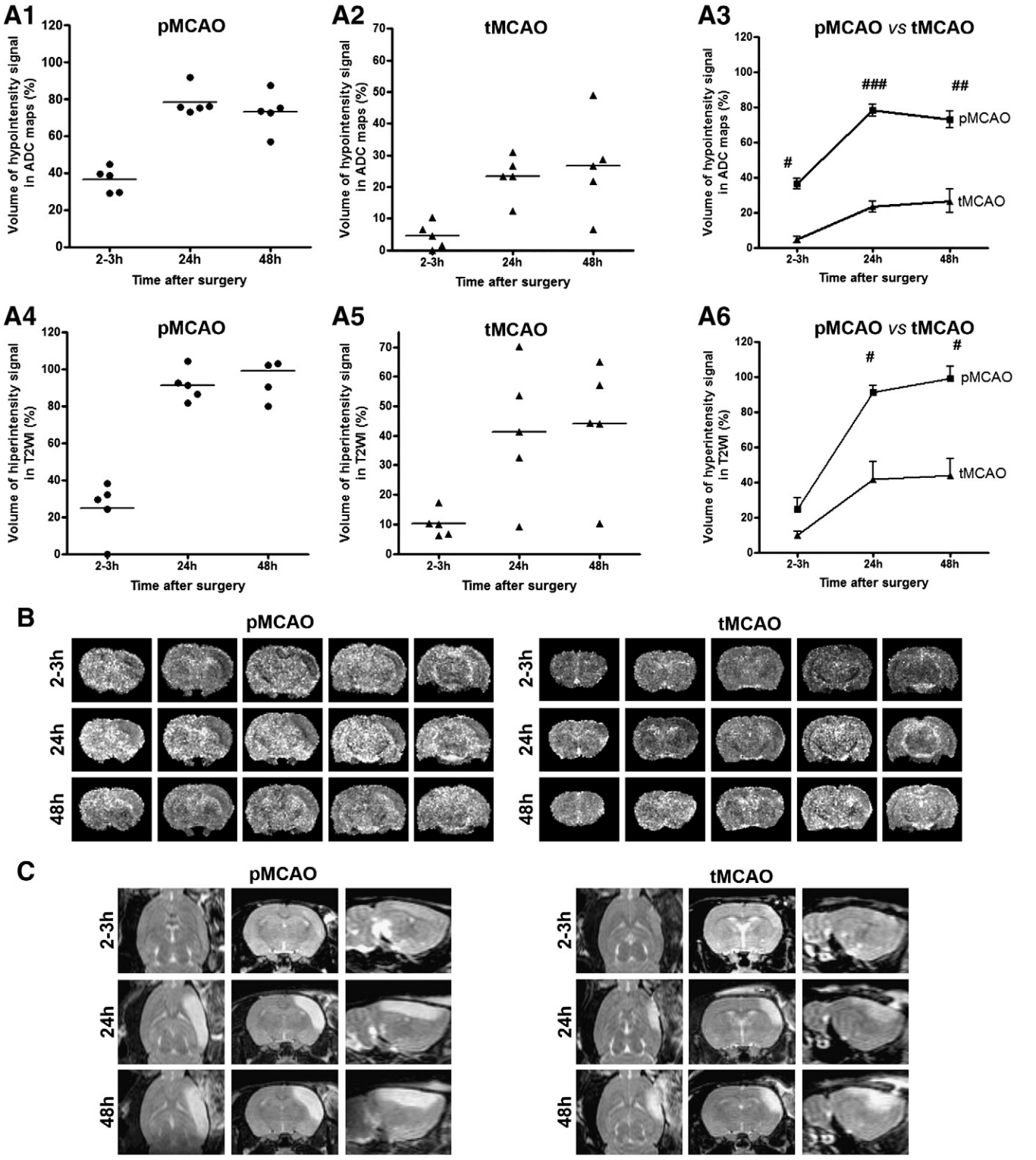

Fig. 2. Study of the cytotoxic edema using ADC maps and vasogenic edema using T2WI in a permanent and a transient model of focal cerebral ischemia. Time course of total cytotoxic and vasogenic edema percentages measured on ADC maps (A1–A3, B) and on T2WI (A4–A6, C), respectively after pMCAO and tMCAO focal cerebral ischemia. The ratio of cortical edema volume in each time *vs*. ipsilateral cortex volume before ischemia was calculated and expressed as percentage. Comparison of the time course of edema size measured on ADC maps (A3) and on T2WI (A6) in both models. A1–2 and A4–5 represent individual cases. Representative images of ADC map (B) and T2WI (C) in tMCAO and pMCAO at different times studied after surgery are shown (2–3, 24 and 48 h). $^{\#,\#\#,\#\#\#}P<0.05$, 0.01, 0.001 *vs.* tMCAO, 2 way ANOVA followed by post hoc Bonferroni's test. Data represent mean ± SEM; N = 5.

(ischemic penumbra) defined as a tissue that will not be infarcted with the presence of reperfusion.

Our results show that the recoverable tissue may be identified by changes on ^{18}F-FDG values maintaining similar ADC and CBF ratios. ^{18}F-FDG values are higher than those found in the recruited tissue – a tissue that will be infarcted at the latest time regardless of the presence of reperfusion – and lower than those in the non-infarcted tissue. These results indicate that, in this context, ^{18}F-FDG PET is the most sensitive approach to identify at early times the recoverable tissue after a mild ischemic episode.

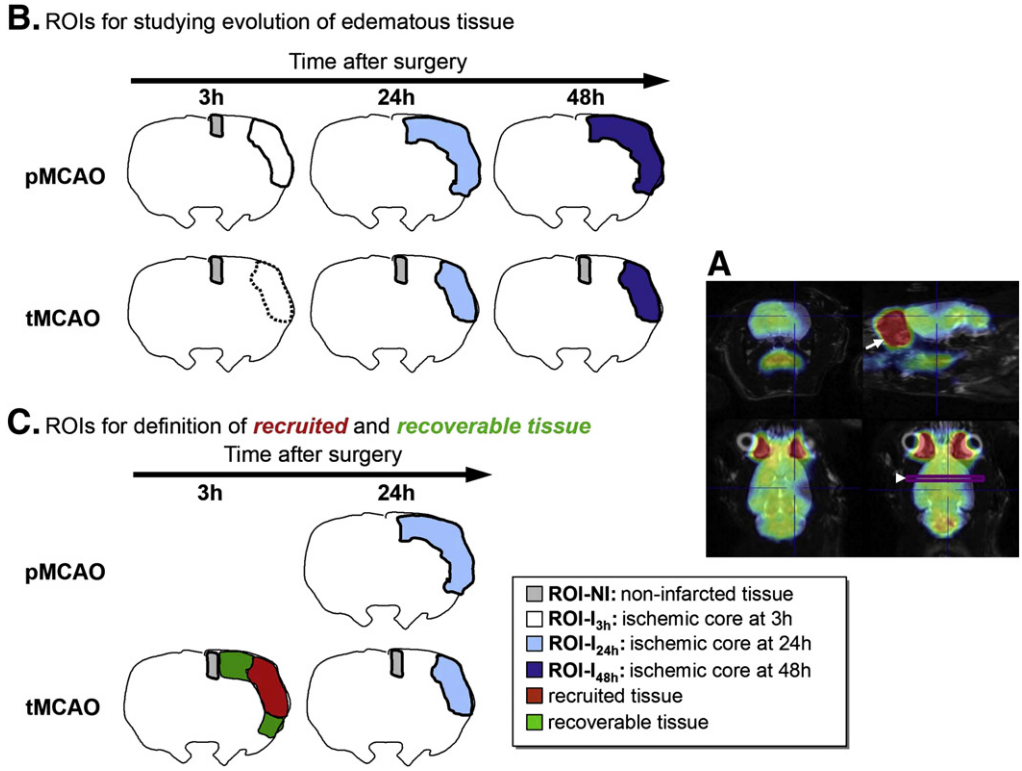

Fig. 3. Definition of regions of interest (ROI). A. Representative orthogonal planes of ^{18}F-FDG PET images co-registered with MR images T2WI3D from a permanent ischemic rat. Regions of interest (ROIs) were manually defined over the ADC map image of one slice selected (Bregma 0, indicated by head row) and at the times indicated in panels B and C. They were applied subsequently over the ADC map, to calculate ADC values, over the PET, for the quantitative analysis of ^{18}F-FDG and over the PWI images, for the quantitative analysis of CBF. B, ROIs for studying evolution of edematous tissue. The tracing used for ROI-I_{3h} in tMCAO, indicated by a discontinuous line, corresponds to the one delineated at 24 h in the same animal (ROI-I_{24h}) (see Materials and methods for details). C, ROIs for definition of recruited and recoverable tissues. Harderian glands are indicated with a row.

Several approaches have been used to discriminate ischemic penumbra. In clinical practice, the penumbra has been estimated by using PWI/DWI mismatch (Neumann-Haefelin et al., 1999; Rohl et al., 2001), PET with ^{15}O tracers (Baron et al., 1984; Sobesky et al., 2005), clinical-DWI mismatch (Davalos et al., 2004; Prosser et al., 2005) and perfusion computed tomography (Hellier et al., 2006; Parsons et al., 2005; Wintermark et al., 2007), among others (Heiss and Sorensen, 2009). However, there are still controversies on what the best approach is. We therefore decided to tackle this issue by using ^{18}F-FDG PET and MRI together. Firstly, PET has been widely used for research and in particular, ^{18}F-FDG has become the most widely used PET radiopharmaceutical in the clinical imaging of oncologic, cardiac and neurologic applications (for review see Hoh, 2007). Furthermore, ^{18}F-FDG PET seems appropriate for the study of recruited (irreversibly injured)/recoverable tissues since this radiotracer is a marker of glucose metabolic activity and reduced glucose metabolism has been described as related to irreversible injury (Zhao et al., 1997). On the other hand, DWI is used in clinical practice to determine the extent of cytotoxic edema (Butcher et al., 2005), provides information about the self-diffusion of water and allows detection of ischemic injury within a few minutes of onset. In this context, we have used ADC maps (obtained from DWI data) to measure infarct volume since they reflect subacute expansion of damage more accurately than DWI hyperintensities, due the "T2 shine-through" effect (Abe et al., 2003). In addition, we have also measured cerebral blood flow using ASL for the PWI since this technique does not require contrast agents and is therefore non-invasive, although it provides low contrast-to-noise ratio and complications for multi-slice approaches (Abe et al., 2003).

One of the objectives of this work was to obtain experimentally different degrees of ischemic damage, in order to differentially establish an area recoverable with reperfusion that could be identified by imaging techniques. For this reason, we have used two models of focal cerebral ischemia, permanent and transient, in such a way that the early reperfusion of occluded vessels in the transient one produced a mild infarct whereas severe damage was caused by permanent occlusion. Moreover, early reperfusion produced no clear injury in ADC maps at the earliest time studied (2–3 h).

In the permanent model (without reperfusion), the reduction in metabolic activity, measured as ^{18}F-FDG uptake, runs parallel to ADC and CBF values at 2–3 h after surgery. This reduction in glucose metabolism was more evident at 24–48 h after injury, which might be attributable to reduced metabolic requirement due to cell death by permanent occlusion. The reduction in ADC values was observed mainly at shorter times (2–3 to 24 h) after surgery, which has been associated with histological signs of irreversible damage (Pierpaoli et al., 1993). The rounded neurons with pale nuclei and swollen cytoplasm mostly observed at 3 h after surgery in our permanent ischemia model correlated well with the ADC reduction observed at this time. However, at later times (24 to 48 h), the development of vasogenic edema and cell lysis, which enlarges the extracellular space, are likely responsible for the subsequent increase in ADC values, as previously described (Abe et al., 2003).

However, in the transient model (early reperfusion), the reduction in ^{18}F-FDG values is associated with normal values of ADC and CBF ratios at 3 h of reperfusion. A short period of ischemia (75 min) followed by an early reperfusion is able to produce a reduction in metabolic activity – despite glucose and oxygen being available – that we can identify using ^{18}F-FDG PET.

ROIs definition on ADC maps is based on the reduction of ADC values. Early reperfusion did not produce a clear edematous core at 2–3 h in this study but the lesion was clearly found at 24 h in all cases. Then, the tracing used for ROI-I_{3h} corresponds to the one delineated at 24 h in the same animal (ROI-I_{24h}); this experimental approach demonstrates that,

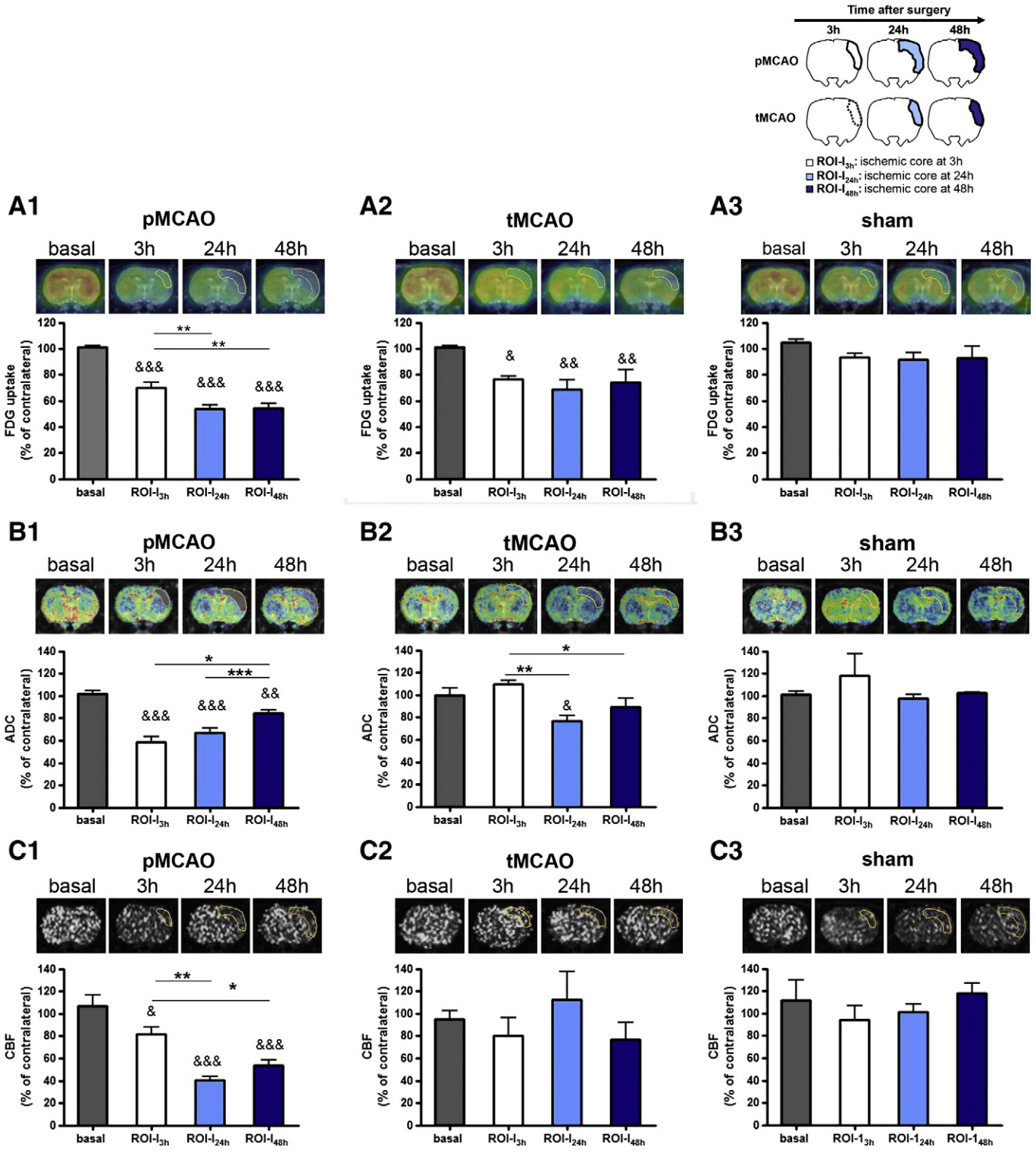

Fig. 4. Study of the edematous tissue by using ^{18}F-FDG uptake, ADC and CBF values in a permanent and a transient model of focal cerebral ischemia. ^{18}F-FDG PET, ADC maps and CBF were co-registered with 3D T2WI MRI images for illustration of anatomical regions. Then, regions of interest (ROIs) were defined for each rat on ADC maps in the ipsilateral cortex, and symmetrical ROIs were drawn in the homologous contralateral regions (see Materials and methods for details). The ^{18}F-FDG uptake, ADC and CBF ratios (ipsilateral *vs.* contralateral) were calculated and multiplied by 100. The tracing used for ROI-I_{3h} in tMCAO corresponds to the one delineated at 24 h in the same animal (ROI-I_{24h}). A1, A2, A3, FDG uptake in the infarcted areas at 3, 24 and 48 h after surgery in permanent (pMCAO), transient (tMCAO) and sham groups, respectively. B1, B2, B3, ADC ratio in the infarcted areas at 3, 24 and 48 h after surgery in pMCAO, tMCAO and sham groups, respectively. C1, C2, C3, CBF ratio in the infarcted areas at 3, 24 and 48 h after surgery in pMCAO, tMCAO and sham groups, respectively. ROIs drawn in the sham group were chosen of a random ischemic rat. Representative coronal ^{18}F-FDG PET images showing the uptake of the tracer, ADC maps and PWI images with the time after the end of surgery (3 h, 24 h and 48 h) in the pMCAO, tMCAO and sham groups as located on each graphic. $^{\&,\&\&,\&\&\&}P<0.05, 0.01, 0.001$ *vs.* basal; $^{*,**,***}P<0.5, 0.01, 0.001$ as indicated (repeated measures ANOVA plus Newman–Keuls test). Data represent mean ± SE; N = 5 for pMCAO and tMCAO groups, N = 3 for sham group.

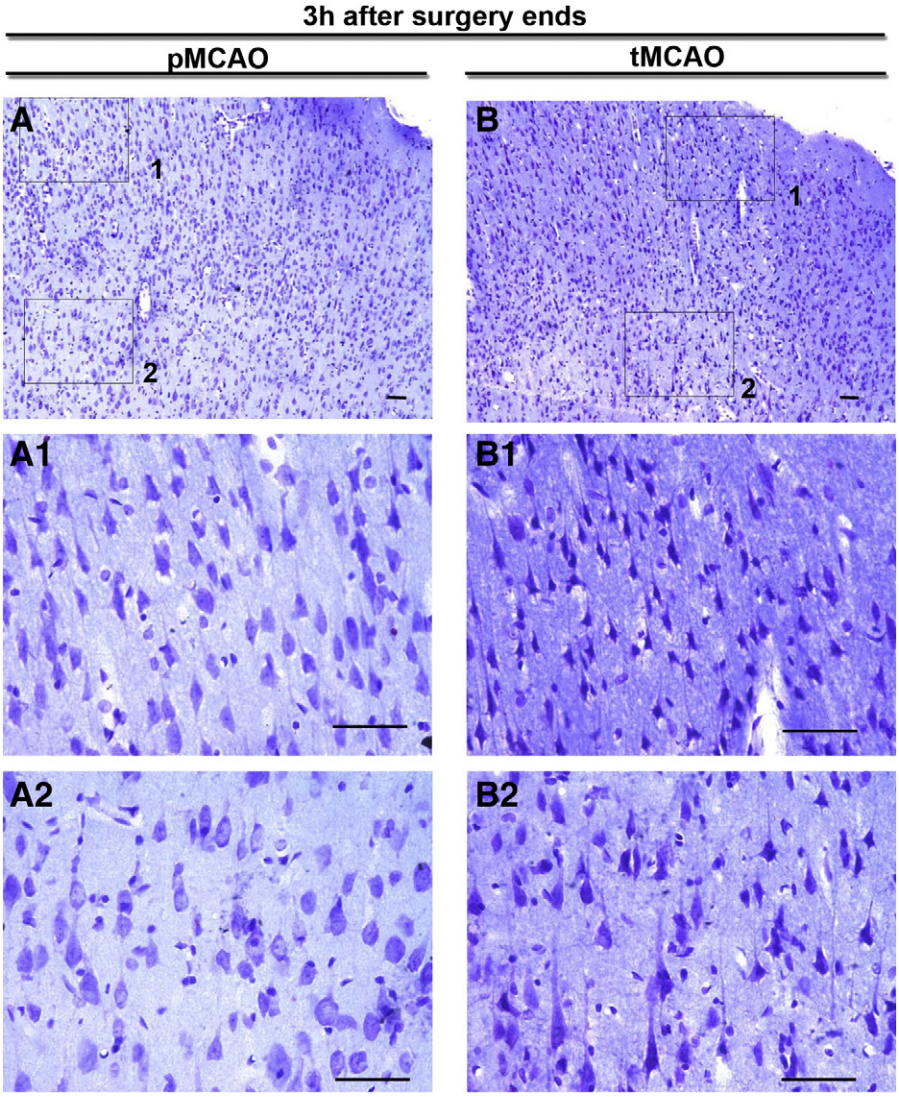

Fig. 5. Early histological changes of cortical lesion after permanent and transient focal cerebral ischemia. A. A representative Nissl-stained coronal brain section at level of Bregma 0 at 3 h after surgery is shown in pMCAO (A) and tMCAO (B) in the territory of the MCA occluded. B. Enlargement of squares in A showing the morphology cells in the enumerated areas. Rounded neurons with pale nuclei and swollen cytoplasm were mainly observed after pMCAO (A1, A2) and triangular morphology and marked condensed nucleus with reduced size of neuronal cell body was mostly observed after tMCAO (B1, B2). Bar 50 μm.

in our transient ischemia model at 2–3 h after surgery, the ischemic area defined is a "tissue at risk" which will be infarcted regardless of the presence of reperfusion (recruited tissue), although no clear hypointensity signal in ADC maps exists.

In experimental focal ischemia, the degree of ADC reduction depends on both the anatomic localization and the duration of the occlusion. Indeed, in agreement with our data showing that ADC values are not significantly affected at 3 h after surgery in the transient model, other authors have found that ADC values return to basal levels or partially recover at early reperfusion (Minematsu et al., 1992); whereas when occlusion time exceeds 2 h, no recovery in ADC is found until 2 to 7 days of reperfusion (Jiang et al., 1993; Neumann-Haefelin et al., 1999). Moreover, neuronal cell retraction mainly observed at 3 h after surgery in the transient ischemia could contribute to the non-reduction of the ADC at this time by increasing the extracellular space. The ADC recovery after early reperfusion does not mean, in our conditions, that histological normalization has occurred. This ADC recovery was followed by a secondary decline in ADC values and neuronal death, as previously described (Neumann-Haefelin et al., 2000; Olah et al., 2001).

Similarly to what occurs with ADC values, a recovery of the CBF was observed with the complete de-occlusion of vessels, suggesting efficient recanalization and no major vascular injury. This result is in agreement with a previous report that shows no changes of CBF by Gadolinium-DTPA at 4.5 h after reperfusion using a 3 vessel occlusion model of ischemia (Lin et al., 2002). However, other authors found no evidence of immediate CBF recovery but observed a strong hyperperfusion in the ipsilateral cortex after 80 min of MCAO using the intraluminal model followed by 2 to 4 days of reperfusion (Wang et al., 2002). Although we observed a slight and transitory CBF increase at 24 h, it did not reach statistical significance. These differences could be attributed to different degrees of damage severity and extension of lesion by reperfusion in the intraluminal model.

Consequently, a concerted monitoring of the variations in local brain glucose utilization (^{18}F-FDG), ADC and CBF that result from focal cerebral ischemia might therefore be useful to assess the severity of the ischemic injury related with early reperfusion or the permanent model of ischemia; in other words, comparison between ^{18}F-FDG, ADC and CBF values allows us to discriminate whether a tissue has undergone early reperfusion (low FDG, but normal ADC and CBF) or permanent ischemia (low FDG, ADC and CBF).

Focusing on the concept of penumbra as an ischemic tissue neighboring regions irreversibly damaged but able to be recovered by

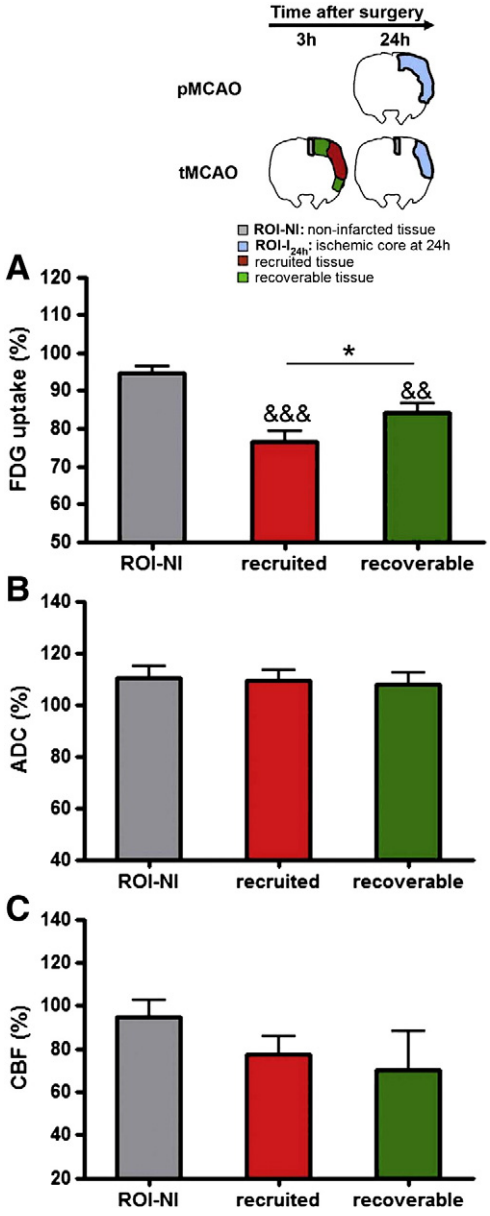

Fig. 6. Study of recruited and recoverable tissue by using ^{18}F-FDG uptake, ADC and CBF values in a transient focal ischemia model. Regions of interest (ROIs) were defined for each rat on ADC maps in the ipsilateral cortex, and symmetrical ROIs were drawn in the homologous contralateral regions. The ^{18}F-FDG, ADC and CBF ratios (ipsilateral *vs*. contralateral) were calculated and multiplied by 100. ^{18}F-FDG (A), ADC (B) and CBF (C) ratios measured at 3 h after surgery in the non-infarcted tissue (ROI-NI), the recruited tissue that progress to infarction in the tMCAO at 24 h; and the recoverable tissue or border that recovers with reperfusion (calculated as recoverable tissue = ROI-$I_{24h\ pMCAO}$-ROI-$I_{24h\ tMCAO}$) (see Materials and methods for details). $^{\&\&,\&\&\&}P<0.01$, 0.001 *vs.* ROI-NI and $^{*}P<0.05$ as indicated (1-way ANOVA plus Newman–Keuls). Data represent mean ± SE; N = 5.

reperfusion, our results demonstrate the existence of another "tissue at risk" which, however, is susceptible of recuperation when occluded arterial vessels are reperfused – recoverable tissue – and may be identified by ^{18}F-FDG values. Indeed, we have found that recoverable tissue is characterized by (1) higher ^{18}F-FDG values than those seen in the recruited tissue but lower than those from the non-infarcted tissue (ROI-NI) and (2) ADC and CBF values which were not significantly different from the other tissues areas.

To our knowledge, this is the first time that a study has approached systematically the characterization of different degrees of ischemic damage by using these three neuroimaging techniques. Our finding showing a mild fall in glucose metabolism associated with the recoverable tissue is in agreement with recent data showing that moderate glucose hypometabolism is related to a peripheral region to the ischemic core that does not develop infarction later on in an intraluminal filament MCAO model (Martin et al., 2009). An interesting hypothesis posed by these authors is that there may exist a threshold of glucose hypometabolism capable of differentiating viable from non-viable tissue. This behavior of the recoverable tissue has also been described in metabolic studies: Thoren et al.(2006) described changes in ^{14}C-glucose metabolism that were not restricted to tissue that developed infarction in a transient model of ischemia. Similarly, Haberg et al., (2006) showed reduced glucose metabolism after reperfusion in areas considered as viable, in a study in which rats subjected to 120 min of ischemia/reperfusion received an iv bolus injection of [1-^{13}C] glucose plus [1,2-^{13}C] acetate. In contrast, an early study using a thromboembolic stroke model in primates showed that in regions surrounding the ischemic core consistent with the penumbral zone, the cerebral metabolic rate of glucose determined with ^{18}F-FDG was increased when measured at 24 h (Kuge et al., 2001). This apparent discrepancy with our results might be due to the fact that our measurement was performed at earlier times after the occlusion; although these authors did not measure glucose metabolism at earlier times, they did find an increase in CBF 1 h after the embolization.

PWI/DWI mismatch has been proposed for assessment of ischemic penumbra. However, lesion based on DWI or PWI (Engelter et al., 2008; Lin et al., 2002; Rojas et al., 2006) is not always detectable in the first few hours after ischemia onset. Small lesion size, small cortical lesions and DWI performed within a few hours after stroke were related to a risk of false-negative DWI-images, suggesting that the diagnosis of acute ischemic stroke cannot be excluded on the base of DWI without visible lesions (Engelter et al., 2008).

Restoration of CBF and no clear hypointensity signal on ADC maps after withdrawal of the suture was observed in our model. Although the recoverable tissue shows a light hypoperfusion without statistical significance, very importantly, our results show that ^{18}F-FDG allows early characterization of this recoverable area when the reperfusion occurs independently, with no clear changes visible on DWI and/or PWI.

Despite all this, our study presents some limitations. It is known that all neuroimaging techniques in spite their increasing technology, still present some limits in spatial or temporal resolution. Specific to our study are other problems such as the delay between MRI and PET images acquisition, or the long time periods required for both preparation and uptake of ^{18}F-FDG. In addition, there are factors that may hinder translationality of our results, such as: the animal model used, changes in cerebrovascular structure modifying vasoreactivity, the heterogeneity of cerebral ischemia (age, infarct volume, time post-ischemia, *etc*.…) and the relationship between brain function and clinical measures, which might also modify the interpretation of our imaging data.

In summary, two possible "tissues at risk" can be defined using a tracer ^{18}FDG PET and MRI techniques: a *recruited tissue*, which will eventually result infarcted, regardless of the presence of reperfusion, and a *recoverable tissue*, which can be salvaged if the early reperfusion occurs. Therefore, ^{18}F-FDG PET appears as a sensitive approach to identify the recoverable tissues at early times, whereas CBF and DWI, by themselves, provide little predictive information in this setting. The early detection of this potentially recoverable tissue after ischemic stroke is of particular interest in the human clinical setting, as a crucial step for appropriate (thrombolytic or not) treatment selection of patients with ischemic stroke. Although for this purpose we have defined areas susceptible to suffer or not suffer infarction with reperfusion through a retrospective study based on a visual analysis and ROIs drawn, future studies are needed at the voxel level before they can be applied clinically.

Acknowledgments

This work was supported by grants from Spanish Ministry of Science and InnovationSAF2009-08145 (MAM), SAF2008-03122 (IL),

from Community of Madrid S-BIO-0170/2006 and from Spanish Ministry of Health RENEVAS RD06/0026/0001 (JS-P) and RD06/0026/0005 (IL). MS is funded by S-BIO-0170/2006.

References

Abe, O., Aoki, S., Shirouzu, I., Kunimatsu, A., Hayashi, N., Masumoto, T., Mori, H., Yamada, H., Watanabe, M., Masutani, Y., Ohtomo, K., 2003. MR imaging of ischemic penumbra. Eur J Radiol 46, 67–78.

Adams Jr., H.P., Brott, T.G., Furlan, A.J., Gomez, C.R., Grotta, J., Helgason, C.M., Kwiatkowski, T., Lyden, P.D., Marler, J.R., Torner, J., Feinberg, W., Mayberg, M., Thies, W., 1996. Guidelines for thrombolytic therapy for acute stroke: a supplement to the guidelines for the management of patients with acute ischemic stroke. A statement for healthcare professionals from a Special Writing Group of the Stroke Council, American Heart Association. Circulation 94, 1167–1174.

Astrup, J., Symon, L., Branston, N.M., Lassen, N.A., 1977. Cortical evoked potential and extracellular K+ and H+ at critical levels of brain ischemia. Stroke 8, 51–57.

Balcerzyk, M., Kontaxakis, G., Delgado, M., Garcia-Garcia, L., Correcher, C., Gonzalez, A.J., Gonzalez, A., Rubio, J.L., Benlloch, J.M., Pozo, M.A., 2009. Initial performance evaluation of a high resolution Albira small animal positrón emission tomography scanner with monolithic crystals and depth-of-interaction encoding from a user's perspective. Meas Sci Technol 20.

Bandera, E., Botteri, M., Minelli, C., Sutton, A., Abrams, K.R., Latronico, N., 2006. Cerebral blood flow threshold of ischemic penumbra and infarct core in acute ischemic stroke: a systematic review. Stroke 37, 1334–1339.

Baron, J.C., Rougemont, D., Soussaline, F., Bustany, P., Crouzel, C., Bousser, M.G., Comar, D., 1984. Local interrelationships of cerebral oxygen consumption and glucose utilization in normal subjects and in ischemic stroke patients: a positron tomography study. J Cereb Blood Flow Metab 4, 140–149.

Butcher, K.S., Parsons, M., MacGregor, L., Barber, P.A., Chalk, J., Bladin, C., Levi, C., Kimber, T., Schultz, D., Fink, J., Tress, B., Donnan, G., Davis, S., 2005. Refining the perfusion–diffusion mismatch hypothesis. Stroke 36, 1153–1159.

Chen, S.T., Hsu, C.Y., Hogan, E.L., Maricq, H., Balentine, J.D., 1986. A model of focal ischemic stroke in the rat: reproducible extensive cortical infarction. Stroke 17, 738–743.

Davalos, A., Blanco, M., Pedraza, S., Leira, R., Castellanos, M., Pumar, J.M., Silva, Y., Serena, J., Castillo, J., 2004. The clinical-DWI mismatch: a new diagnostic approach to the brain tissue at risk of infarction. Neurology 62, 2187–2192.

Engelter, S.T., Wetzel, S.G., Bonati, L.H., Fluri, F., Lyrer, P.A., 2008. The clinical significance of diffusion-weighted MR imaging in stroke and TIA patients. Swiss Med Wkly 138, 729–740.

Haberg, A., Qu, H., Sonnewald, U., 2006. Glutamate and GABA metabolism in transient and permanent middle cerebral artery occlusion in rat: importance of astrocytes for neuronal survival. Neurochem Int 48, 531–540.

Hacke, W., Kaste, M., Bluhmki, E., Brozman, M., Davalos, A., Guidetti, D., Larrue, V., Lees, K.R., Medeghri, Z., Machnig, T., Schneider, D., von Kummer, R., Wahlgren, N., Toni, D., 2008. Thrombolysis with alteplase 3 to 4.5 hours after acute ischemic stroke. N Engl J Med 359, 1317–1329.

Heiss, W.D., Sorensen, A.G., 2009. Advances in imaging. Stroke 40, e313–e314.

Hellier, K.D., Hampton, J.L., Guadagno, J.V., Higgins, N.P., Antoun, N.M., Day, D.J., Gillard, J.H., Warburton, E.A., Baron, J.C., 2006. Perfusion CT helps decision making for thrombolysis when there is no clear time of onset. J Neurol Neurosurg Psychiatry 77, 417–419.

Hoh, C.K., 2007. Clinical use of FDG PET. Nucl Med Biol 34, 737–742.

Jiang, Q., Zhang, Z.G., Chopp, M., Helpern, J.A., Ordidge, R.J., Garcia, J.H., Marchese, B.A., Qing, Z.X., Knight, R.A., 1993. Temporal evolution and spatial distribution of the diffusion constant of water in rat brain after transient middle cerebral artery occlusion. J Neurol Sci 120, 123–130.

Kaur, J., Zhao, Z., Klein, G.M., Lo, E.H., Buchan, A.M., 2004. The neurotoxicity of tissue plasminogen activator? J Cereb Blood Flow Metab 24, 945–963.

Kuge, Y., Yokota, C., Tagaya, M., Hasegawa, Y., Nishimura, A., Kito, G., Tamaki, N., Hashimoto, N., Yamaguchi, T., Minematsu, K., 2001. Serial changes in cerebral blood flow and flow-metabolism uncoupling in primates with acute thromboembolic stroke. J Cereb Blood Flow Metab 21, 202–210.

Lin, T.N., Sun, S.W., Cheung, W.M., Li, F., Chang, C., 2002. Dynamic changes in cerebral blood flow and angiogenesis after transient focal cerebral ischemia in rats. Evaluation with serial magnetic resonance imaging. Stroke 33, 2985–2991.

Liu, T.H., Beckman, J.S., Freeman, B.A., Hogan, E.L., Hsu, C.Y., 1989. Polyethylene glycol-conjugated superoxide dismutase and catalase reduce ischemic brain injury. Am J Physiol 256, H589–H593.

Lo, E.H., 2008. A new penumbra: transitioning from injury into repair after stroke. Nat Med 14, 497–500.

Lou, M., Zhang, H., Wang, J., Wen, S.Q., Tang, Z.Q., Chen, Y.Z., Yan, W.Q., Ding, M.P., 2007. Hyperbaric oxygen treatment attenuated the decrease in regional glucose metabolism of rats subjected to focal cerebral ischemia: a high resolution positron emission tomography study. Neuroscience 146, 555–561.

Martin, A., Rojas, S., Pareto, D., Santalucia, T., Millan, O., Abasolo, I., Gomez, V., Llop, J., Gispert, J.D., Falcon, C., Bargallo, N., Planas, A.M., 2009. Depressed glucose consumption at reperfusion following brain ischemia does not correlate with mitochondrial dysfunction and development of infarction: an in vivo positron emission tomography study. Curr Neurovasc Res 6, 82–88.

Minematsu, K., Li, L., Sotak, C.H., Davis, M.A., Fisher, M., 1992. Reversible focal ischemic injury demonstrated by diffusion-weighted magnetic resonance imaging in rats. Stroke 23, 1304–1310 discussion 1310–1301.

Neumann-Haefelin, T., Wittsack, H.J., Wenserski, F., Siebler, M., Seitz, R.J., Modder, U., Freund, H.J., 1999. Diffusion- and perfusion-weighted MRI. The DWI/PWI mismatch region in acute stroke. Stroke 30, 1591–1597.

Neumann-Haefelin, T., Kastrup, A., de Crespigny, A., Yenari, M.A., Ringer, T., Sun, G.H., Moseley, M.E., 2000. Serial MRI after transient focal cerebral ischemia in rats: dynamics of tissue injury, blood–brain barrier damage, and edema formation. Stroke 31, 1965–1972 discussion 1972–1963.

Obenaus, A., Ashwal, S., 2008. Magnetic resonance imaging in cerebral ischemia: focus on neonates. Neuropharmacology 55, 271–280.

Olah, L., Wecker, S., Hoehn, M., 2001. Relation of apparent diffusion coefficient changes and metabolic disturbances after 1 hour of focal cerebral ischemia and at different reperfusion phases in rats. J Cereb Blood Flow Metab 21, 430–439.

Parsons, M.W., Pepper, E.M., Chan, V., Siddique, S., Rajaratnam, S., Bateman, G.A., Levi, C. R., 2005. Perfusion computed tomography: prediction of final infarct extent and stroke outcome. Ann Neurol 58, 672–679.

Pierpaoli, C., Righini, A., Linfante, I., Tao-Cheng, J.H., Alger, J.R., Di Chiro, G., 1993. Histopathologic correlates of abnormal water diffusion in cerebral ischemia: diffusion-weighted MR imaging and light and electron microscopic study. Radiology 189, 439–448.

Prosser, J., Butcher, K., Allport, L., Parsons, M., MacGregor, L., Desmond, P., Tress, B., Davis, S., 2005. Clinical-diffusion mismatch predicts the putative penumbra with high specificity. Stroke 36, 1700–1704.

Rohl, L., Ostergaard, L., Simonsen, C.Z., Vestergaard-Poulsen, P., Andersen, G., Sakoh, M., Le Bihan, D., Gyldensted, C., 2001. Viability thresholds of ischemic penumbra of hyperacute stroke defined by perfusion-weighted MRI and apparent diffusion coefficient. Stroke 32, 1140–1146.

Rojas, S., Martin, A., Justicia, C., Falcon, C., Bargallo, N., Chamorro, A., Planas, A.M., 2006. Modest MRI signal intensity changes precede delayed cortical necrosis after transient focal ischemia in the rat. Stroke 37, 1525–1532.

Rojas, S., Herance, J.R., Abad, S., Jimenez, X., Pareto, D., Ruiz, A., Torrent, E., Figueiras, F.P., Popota, F., Fernandez-Soriano, F.J., Planas, A.M., Gispert, J.D., Evaluation of Hypoxic Tissue Dynamics with (18)F-FMISO PET in a Rat Model of Permanent Cerebral Ischemia. Mol Imaging Biol.

Sobesky, J., Zaro Weber, O., Lehnhardt, F.G., Hesselmann, V., Neveling, M., Jacobs, A., Heiss, W.D., 2005. Does the mismatch match the penumbra? Magnetic resonance imaging and positron emission tomography in early ischemic stroke. Stroke 36, 980–985.

Takasawa, M., Beech, J.S., Fryer, T.D., Hong, Y.T., Hughes, J.L., Igase, K., Jones, P.S., Smith, R., Aigbirhio, F.I., Menon, D.K., Clark, J.C., Baron, J.C., 2007. Imaging of brain hypoxia in permanent and temporary middle cerebral artery occlusion in the rat using 18F-fluoromisonidazole and positron emission tomography: a pilot study. J Cereb Blood Flow Metab 27, 679–689.

Thiel, A., Lottgen, J., Grond, M., Pietrzyk, U., Heiss, W.D., 2001. Estimation of regional cerebral blood flow levels in ischemia using [(15)O]water of [(11)C]flumazenil PET without arterial input function. J Comput Assist Tomogr 25, 446–451.

Thoren, A.E., Helps, S.C., Nilsson, M., Sims, N.R., 2006. The metabolism of C-glucose by neurons and astrocytes in brain subregions following focal cerebral ischemia in rats. J Neurochem 97, 968–978.

Wang, L., Yushmanov, V.E., Liachenko, S.M., Tang, P., Hamilton, R.L., Xu, Y., 2002. Late reversal of cerebral perfusion and water diffusion after transient focal ischemia in rats. J Cereb Blood Flow Metab 22, 253–261.

Wintermark, M., Meuli, R., Browaeys, P., Reichhart, M., Bogousslavsky, J., Schnyder, P., Michel, P., 2007. Comparison of CT perfusion and angiography and MRI in selecting stroke patients for acute treatment. Neurology 68, 694–697.

Zhao, W., Belayev, L., Ginsberg, M.D., 1997. Transient middle cerebral artery occlusion by intraluminal suture: II. Neurological deficits, and pixel-based correlation of histopathology with local blood flow and glucose utilization. J Cereb Blood Flow Metab 17, 1281–1290.